Photochemical & Photobiological Sciences

www.rsc.org/pps

PAPER

The role of humic acid aggregation on the kinetics of photosensitized singlet oxygen production and decay†

Luciano Carlos,[a] Brian W. Pedersen,[b] Peter R. Ogilby*[b] and Daniel O. Mártire*[a]

Received 4th January 2011, Accepted 28th February 2011
DOI: 10.1039/c1pp00003a

The effect of humic acid (HA) aggregate formation on the photosensitized generation and subsequent quenching of singlet molecular oxygen $O_2(a^1\Delta_g)$ was investigated. Time-resolved $O_2(a^1\Delta_g)$ phosphorescence traces were obtained from (a) bulk samples of HA dispersions and (b) microscope-based experiments performed upon irradiation of a single HA aggregate. In the bulk experiments, the dependence of the $O_2(a^1\Delta_g)$ lifetime on the HA concentration yields a critical concentration for the formation of micrometric HA aggregates of 0.58 g L^{-1}. This value is consistent with that obtained using pyrene as a fluorescent probe (0.38 g L^{-1}). Microscope-based experiments were also performed with HA samples containing added singlet oxygen sensitizers; either the hydrophobic *meso*-tetraphenylporphyrin (TPP) or the hydrophilic 5,10,15,20-tetrakis(*N*-methyl-4-pyridyl)-21*H*,23*H*-porphine (TMPyP). Singlet oxygen phosphorescence could only be detected upon irradiation of TMPyP, a molecule which localizes on the exterior part of the HA aggregates. The inability to detect $O_2(a^1\Delta_g)$ phosphorescence from HA samples containing TPP is consistent with the model that the $O_2(a^1\Delta_g)$ produced in the interior of the aggregate was completely quenched by the high local concentration of HA reactive groups in this environment.

Introduction

In aquatic ecosystems, singlet molecular oxygen, $O_2(a^1\Delta_g)$, is considered to be important in the photochemical degradation or modification of organic pollutants.[1] Singlet oxygen is the lowest excited electronic state of molecular oxygen, and has a unique chemistry different from that of the triplet ground state of oxygen, $O_2(X^3\Sigma g^-)$.[2,3] The formation of $O_2(a^1\Delta_g)$ in aquatic ecosystems can be achieved by photosensitization. In this process, a molecule (the so-called sensitizer) absorbs sunlight to populate an excited state which, in turn, transfers its energy of excitation to $O_2(X^3\Sigma g^-)$ in a collision-dependent process to produce $O_2(a^1\Delta_g)$.

In natural waters, humic substances (HS) represent the main fraction of dissolved organic carbon that absorb solar radiation and, therefore, they play an important role in aquatic photochemistry.[4] In particular, HS act as $O_2(a^1\Delta_g)$ sensitizers.[1,5–7] Photolysis of HS also leads to the formation of other reactive species including free radicals and hydrated electrons,[8] reactive triplet states,[9,10] hydroxyl radicals,[11,12] superoxide,[13] and hydrogen peroxide,[14,15] all of which play a role in aquatic photochemistry.

Detailed knowledge of the molecular sizes of the HS is essential for understanding their physical-chemical properties and environmental role. Traditional concepts which originated from the supposed observations of large molecular weights,[16,17] postulated that HS were comprised of polymeric macromolecules.[18] However, evidence gathered during the past decade based on a wide range of techniques provide a new view.[19] This alternative perspective indicates the large molecular weights of HS is only apparent and results, rather, from self-assembly of relatively small and heterogeneous humic molecules into large supramolecular species stabilized by weak dispersive forces.[20]

The same interactions that promote supramolecular association also lead to the formation of micrometric micelle-like HS aggregates in which intra- or intermolecular organization produces interior hydrophobic domains separated from the aqueous surroundings by exterior hydrophilic layers.[19,21] Values of the critical micelle concentration (cmc) depend on parameters such as pH, temperature, and the nature of the HS itself. It was recently demonstrated that within the hydrophobic interior of HS, concentrations of $O_2(a^1\Delta_g)$ were 2–3 orders of magnitude higher than that in bulk solution.[22] In this line, Hassett proposed that the chromophoric dissolved organic matter acts as a microreactor that could enhance the reactivity of a contaminant by bringing it into close association with photochemically produced $O_2(a^1\Delta_g)$.[23]

[a]*Instituto de Investigaciones Fisicoquímicas Teóricas y Aplicadas (INIFTA), CCT-La Plata-CONICET, Universidad Nacional de La Plata, Casilla de correo 16, sucursal 4 (1900), La Plata, Argentina. E-mail: dmartire@inifta.unlp.edu.ar; Fax: +54 221 4254642; Tel: +54 221 4257430/7291*

[b]*Center for Oxygen Microscopy and Imaging (COMI), Department of Chemistry, University of Aarhus, Aarhus, Denmark. E-mail: progilby@chem.au.dk; Fax: +45 8619 6199; Tel: +45 8942 3863*

† Electronic supplementary information (ESI) available: Porphyrin structures, a plot of the time-resolved $O_2(a^1\Delta_g)$ phosphorescence signal *vs.* C_{HA}, microscope images of HA suspension with different washed conditions and controls for the $O_2(a^1\Delta_g)$ microscope-based experiments. See DOI: 10.1039/c1pp00003a

In light of such HS aggregate formation and the fact that HS sensitized $O_2(a^1\Delta_g)$ production plays an important role in aquatic photochemistry, it is imperative that one characterize $O_2(a^1\Delta_g)$ behavior as a function of HS aggregation over a wide range of HS concentrations. We thus set out to investigate the extent to which aggregation of humic acids (HA) influence the kinetics of $O_2(a^1\Delta_g)$ formation and deactivation. Studies were performed using (a) bulk samples contained in a cuvette, and (b) spatially-resolved, microscope-based experiments. The data obtained indicate that HS structure indeed influences the behavior of $O_2(a^1\Delta_g)$.

Experimental

Materials

Aldrich humic acid sodium salt was employed in our experiments. Although this humic acid has its limitations as a model for dissolved organic matter present in natural waters,[24] we chose this material because of its relatively high molecular weight, its close correspondence to soil organic matter, its reported supramolecular structure in aqueous solution[22] and because it was previously used in fluorescence quenching studies, which have demonstrated associations between hydrophobic compounds and macromolecular organic matter.[25,26]

meso-Tetraphenylporphyrin (TPP) and 5,10,15,20-tetrakis(*N*-methyl-4-pyridyl)-21*H*,23*H*-porphine (TMPyP), whose structures are given in the ESI (Fig. S1),† were obtained from Porphyrin Systems. Deionized water was obtained from a Millipore system.

Instrumentation

Absorption spectra were recorded using a Shimadzu model 3600 UV-Vis-NIR spectrometer. Fluorescence measurements were made using a Jobin–Yvon SPEX Fluorolog spectrofluorometer (model FL3-11) equipped with a steady-state Xe lamp as the excitation source. The fluorescence spectra of pyrene were recorded from 350 to 550 nm with excitation at 337 nm. The slit widths for both excitation and emission were set to yield a spectral resolution of 3 nm.

Microscope images were obtained using an Olympus IX70 inverted microscope (60× water-immersion objective). Fluorescence images were performed by irradiating the sample with a steady-state Xe lamp, using interference filters to select the appropriate excitation wavelength (λ_{exc} = 420 nm). Light emitted by the sample was detected through interference filters (λ_{em} = 650 nm) using a CCD camera (Evolution QEi controlled by ImagePro software, Media Cybernetics) placed at the image plane of the microscope. Bright-field images were recorded using the same CCD camera, and backlighting was achieved with a tungsten lamp. The ratiometric images were obtained using ImageJ software.

$O_2(a^1\Delta_g)$ measurements were performed using instrumentation that has been described previously.[27–31] Briefly, the 840 nm output of a femtosecond laser was amplified and then frequency-doubled to 420 nm with a beta barium borate crystal. Experiments with bulk samples were performed in 1 cm pathlength cuvettes using the collimated output of the femtosecond laser as the excitation source. The $O_2(a^1\Delta_g)$ phosphorescence intensity obtained from the cuvette was measured by placing a 1275 nm interference filter in front of a cooled photomultiplier (PMT, Hamamatsu model R5509-42) which was used in a photon counting mode. The PMT was cooled to −80 °C by a flow of gaseous nitrogen that had been pumped through a dewar of liquid nitrogen. Experiments were performed using the unfocused output of the laser (beam diameter ~ 7 mm) operated at a repetition rate of 1 kHz such that 5 μJ pulse^{-1} were delivered to the sample. In the microscope experiments, the samples were placed in an atmosphere-controlled chamber that was mounted on the translation stage of the microscope. The output of the femtosecond laser system was focused into the sample using the microscope objective (diameter at the beam waist was ~1 μm). The $O_2(a^1\Delta_g)$ phosphorescence emitted was collected using the microscope objective, spectrally isolated using an interference filter, and transmitted to the photomultiplier tube operated in a photon-counting mode. It should be noted that, although the waist of the focused laser beam at the sample is ~1 μm, singlet oxygen will be generated in a larger spatial domain due to the scattering of the incident light by the sample.[32] The laser was operated at a repetition rate of 1 kHz with an excitation energy of 10 nJ pulse^{-1} delivered to the microscope objective.

Experimental protocols

Determination of cmc using pyrene as a probe. Pyrene was used as a fluorescent probe to determine the cmc of HA in aqueous medium. In these experiments, pyrene was first dissolved in methanol to a concentration of 2.0 mM. This stock solution was then diluted with deionized water to yield a pyrene concentration of 2 μM. This latter solution was used as a solvent to prepare solutions containing different concentrations of HA, C_{HA}, over the range 0.005–0.9 g L^{-1}. The pH of these solutions ranged from 8.0 to 9.5 depending on C_{HA}. For a solution with a given C_{HA}, the values of I_1/I_3, representing the ratio of the fluorescence intensity of the first (I_1, *ca.* 373 nm) and third (I_3, *ca.* 384 nm) vibronic bands of pyrene, were calculated and plotted against the C_{HA}.[33] The cmc value was derived from the intercepts of the slopes for the rapidly varying part and the nearly horizontal part of the plot.[34] Absorption spectra of the samples were used to correct the I_1/I_3 ratio for both primary and secondary inner filter effects.[35]

$O_2(a^1\Delta_g)$ phosphorescence. *Cuvette experiments*: All the HA suspensions were made in D_2O and sonicated for 20 min. The C_{HA} range studied was 0.06–1.6 g L^{-1} and the pD ranged between 8.5 and 10.5. *Microscope experiments*: Stock solutions of TMPyP in D_2O (A^{420nm} = 1.2), TPP in CH_2Cl_2 (A^{420nm} > 3.5) and HA in D_2O (2.6 g L^{-1}) were prepared. Then, three different dilutions were independently performed as follows: (a) the HA suspension was diluted with D_2O to a concentration of 1.3 g L^{-1}. (b) 5 mL of the TMPyP stock solution was added to 5 mL of the HA suspension. (c) 20 μL of the TPP stock solution and 5 mL of D_2O were added to 5 mL of the HA suspension. The remaining concentration of CH_2Cl_2 (0.2%) in the HA-TPP solutions was considered not to affect the self-aggregation behavior of HA.

In the three suspensions described above, both the C_{HA} (1.3 g L^{-1}) and the pD (around 10) were the same. To measure the $O_2(a^1\Delta_g)$ phosphorescence in the microscope, 20 μL of each suspension were dropped onto cover slips coated with poly-D-lysine and they were left to dry for 3 h at room temperature. Bright-field microscope images of the HA aggregates showed that 3 h was a sufficient time to allow fixation of the aggregate to the cover slips. After drying, 60 μL of D_2O were added to the sample.

During the experiments with focused irradiation, the samples were exposed to an atmosphere of 100% $O_2(X^3\Sigma_g^-)$. Due to the low intensity of the $O_2(a^1\Delta_g)$ phosphorescence signal, the samples were irradiated and data accumulated for 1 h. The aggregates selected to measure $O_2(a^1\Delta_g)$ phosphorescence were bigger than 5 μm in diameter (recall that the beam waist of the focused laser was ~1 μm in diameter, *vide supra*). Bright-field images recorded before and after the irradiation of the sample were used to assess the morphology and the position of a given HA aggregate.

Results and Discussion

HA critical micelle concentration

Fig. 1 shows fluorescence spectra of pyrene recorded in H_2O dispersions of HA at different concentrations of HA, C_{HA}. For this experiment, we rely on the fact that the ratio of the corrected intensities of the 373 nm and 384 nm bands of pyrene fluorescence, denoted $(I_1/I_3)_{corr}$, which is larger in polar media and decreases with decreasing polarity, can be used to monitor the microenvironment of pyrene.[33] By monitoring this ratio *vs.* C_{HA}, it is possible to obtain a value for the HA cmc under our experimental conditions (see inset of Fig. 1). In this experiment, a cmc value of 0.38 g L^{-1} was determined.

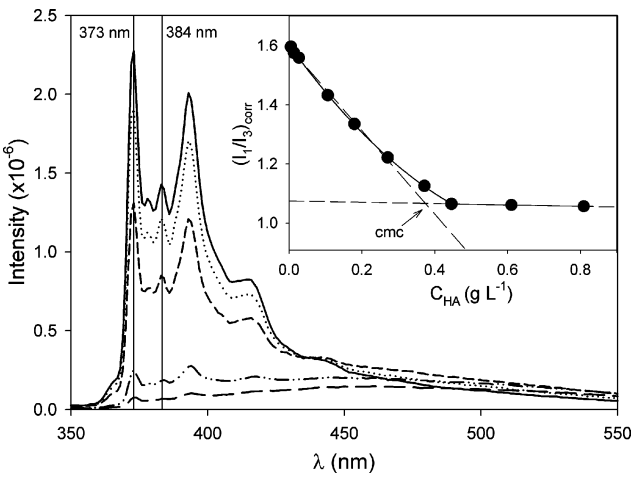

Fig. 1 Fluorescence spectra (λ_{exc} = 337 nm) of a series of aqueous HA samples that contain pyrene (2 μM): From top to bottom C_{HA} = 0.013, 0.027, 0.106, 0.440 and 0.810 g L^{-1}. Vertical lines have been superimposed to identify the bands used to create the ratio I_1/I_3. Inset: Plot of the corrected ratio I_1/I_3 *vs.* C_{HA}.

Fig. 1 shows that, at low C_{HA}, the ratio $(I_1/I_3)_{corr}$ = 1.6, while for C_{HA} > cmc, $(I_1/I_3)_{corr}$ equals 1.06. Saxena *et al.*[36] found a linear correlation between the ratio I_1/I_3 and the dielectric constant of the medium. The values of $(I_1/I_3)_{corr}$ = 1.6 and 1.06 correspond to media with dielectric constants coincident with those of water and a short chain alcohol, such as ethanol or propanol, respectively.

Although Šmejkalová and Piccolo[37] have concluded in an independent NMR study that some of their HA samples (not supplied by Aldrich) showed micelle-like behavior with large cmc values of about 4 g L^{-1}, we show HA aggregation at a much lower concentration, as also observed by Kučerík *et al.* by high resolution ultrasonic spectroscopy.[38]

Bulk $O_2(a^1\Delta_g)$ experiments

To evaluate the effect of HA aggregation on the $O_2(a^1\Delta_g)$ lifetime (τ_Δ), time-resolved $O_2(a^1\Delta_g)$ phosphorescence experiments were performed using bulk samples in cuvettes over the C_{HA} range of 0.06–1.6 g L^{-1}. Fig. 2 shows representative 1275 nm $O_2(a^1\Delta_g)$ phosphorescence traces obtained upon 420 nm irradiation of HA in air-saturated D_2O dispersions containing different amounts of HA. Experiments were performed in D_2O because the lifetime of singlet oxygen in this solvent is ~20 times longer than that in H_2O and, as such, it becomes easier to distinguish the kinetics of singlet oxygen formation from the kinetics of singlet oxygen decay.[2]

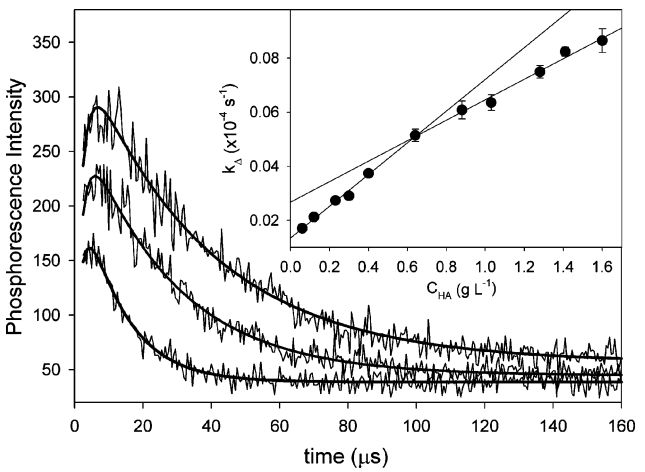

Fig. 2 Time-resolved 1275 nm $O_2(a^1\Delta_g)$ phosphorescence signals sensitized by HA obtained from air-saturated D_2O solutions containing 0.12 g L^{-1} (upper trace), 0.40 g L^{-1} (middle trace), and 1.4 g L^{-1} (lower trace) HA. The solid lines show the fitting of the signals using eqn (1). Inset: Plot of k_Δ *vs.* the concentration of HA. The error bars represent the standard deviation of the data obtained in three independent experiments.

In all cases, the time-dependent phosphorescence intensity, $P(t)$, could be adequately modeled with a difference of two exponential functions, which is in accordance with the triplet state-photosensitized production of singlet oxygen (eqn (1)).[2,39]

$$P(t) = \frac{K}{k_\Delta - k_T} \times (e^{-k_T t} - e^{-k_\Delta t}) \quad (1)$$

$$k_\Delta = (k_q + k_{rxn})[HA] + k_{solv}[solv] \quad (2)$$

In eqn (1), K is a scaling parameter that includes the efficiency of $O_2(a^1\Delta_g)$ production, k_T is the rate constant for all channels of sensitizer triplet state deactivation, and k_Δ is the rate constant that accounts for all channels of singlet oxygen deactivation (*i.e.*, $k_\Delta = 1/\tau_\Delta$). In eqn (2) k_q and k_{rxn} are the rate constants of the physical quenching and chemical reaction channels, respectively, and k_{solv} is the rate constant for $O_2(a^1\Delta_g)$ deactivation by the solvent.

The lifetime of $O_2(a^1\Delta_g)$ in neat D_2O is ~67 μs.[40] At an HA concentration of 0.12 g L^{-1}, we obtain τ_Δ = 47 μs, and at an HA concentration of 1.4 g L^{-1}, τ_Δ = 12 μs (Fig. 2). These data suggest that the HA-sensitized $O_2(a^1\Delta_g)$, which we optically detect is principally located in the aqueous medium and that HA, in turn, also acts as a quencher of this $O_2(a^1\Delta_g)$ population.

In a homogeneous solution containing a dissolved $O_2(a^1\Delta_g)$ quencher, the magnitude of k_Δ generally increases linearly with

an increase in the concentration of the quencher.[2,41] The inset of Fig. 2 shows that the dependence of k_Δ on C_{HA} appears to have two linear regions, one at low C_{HA} and the other at high C_{HA}. These lines intersect at an HA concentration (C_{HA} = 0.58 g L^{-1}) which, given the uncertainties in the respective experiments, is close to the cmc value independently determined using the fluorescence of pyrene (see above). The difference between the slopes at high and low HA concentration could be interpreted to indicate that HA aggregation lowers the quenching rate constant of $O_2(a^1\Delta_g)$ by HA. This phenomenon might reflect the fact that, upon aggregation, fewer HA functional groups are available to interact with $O_2(a^1\Delta_g)$. Related observations have been made with proteins; denaturing the protein exposes reactive functional groups that result in a more efficient deactivation of $O_2(a^1\Delta_g)$.[42]

The slope of each linear region (inset of Fig. 2) equals the corresponding overall bimolecular rate constant ($k_q + k_{rxn}$). The values obtained are $(5.9 \pm 0.3)\times10^4$ L g^{-1} s^{-1} and $(3.8 \pm 0.3)\times10^4$ L g^{-1} s^{-1} at low and high concentrations of HA, respectively. Assuming a molecular weight of 4.7×10^3 for HA,[43] rate constants for $O_2(a^1\Delta_g)$ deactivation of 2.8×10^8 M^{-1} s^{-1} and 1.8×10^8 M^{-1} s^{-1} are obtained for the low and high concentration ranges, respectively. In the least, these data indicate that HA efficiently deactivates and/or reacts with $O_2(a^1\Delta_g)$.

From the (42 ± 1)% C obtained for the same batch of HA employed here,[43] it is also possible to express the quenching constants in units of L mol(C)$^{-1}$ s^{-1}. Values of 1.6×10^6 L mol(C)$^{-1}$ s^{-1} and 1.0×10^6 L mol(C)$^{-1}$ s^{-1} were obtained for the low and high concentration range, respectively. These values are similar to those reported by Cory *et al.*[44] for solutions of pD = 6–7 of Suwannee River and Pony Lake fulvic acids (4.1×10^6 and 1.6×10^6 L mol(C)$^{-1}$ s^{-1}, respectively), but larger than those obtained by Hessler *et al.*[45] for several humic substances with concentrations lower than 0.2 g L^{-1} ($3–4 \times 10^4$ L mol(C)$^{-1}$ s^{-1} for solutions of pD = 9). Cory *et al.*[44] concluded that $O_2(a^1\Delta_g)$ reacts with humic substances with rate constants comparable to phenols, naphthols, or aromatic amines, on a per carbon basis.

Bulk $O_2(a^1\Delta_g)$ experiments with an added quencher

The hydrophilic salt sodium azide, NaN_3, efficiently quenches $O_2(a^1\Delta_g)$ with a rate constant of ~3×10^8 s^{-1} M^{-1}.[46] In separate experiments, this salt was added to our HA solutions and time-resolved $O_2(a^1\Delta_g)$ phosphorescence signals were recorded under conditions where kinetic competition between HA and the added quencher determine the $O_2(a^1\Delta_g)$ lifetime.

NaN_3 is expected to be localized in the bulk aqueous medium. Addition of 1.0 mM NaN_3 to our HA solutions led to complete quenching of the $O_2(a^1\Delta_g)$ phosphorescence for all HA concentrations tested. These results support our suggestion (*vide supra*) that, in these cuvette experiments, we are detecting $O_2(a^1\Delta_g)$ that escapes from the HA supramolecular structures into the D_2O solution. Our results are consistent with a model in which $O_2(a^1\Delta_g)$ inside the HA aggregates is efficiently quenched due to the high local concentration of reactive groups.

Microscope experiments

In the cuvette experiments, HA itself was used as the sensitizer to generate $O_2(a^1\Delta_g)$. Even though the quantum yield of HA-sensitized $O_2(a^1\Delta_g)$ production is low (*ca.* 1–5%),[47] an appreciable $O_2(a^1\Delta_g)$ phosphorescence signal could nevertheless be readily obtained (Fig. 2). However, for spatially-resolved microscope experiments, the irradiated volume of sample is much smaller and the number of $O_2(a^1\Delta_g)$ molecules produced per laser pulse is correspondingly less than in the cuvette experiments. As a result, with our current microscope instrumentation, it was not possible to detect the HA-sensitized $O_2(a^1\Delta_g)$ phosphorescence signal. Because of this limitation, a series of different experiments were designed in which efficient $O_2(a^1\Delta_g)$ sensitizers were added to the HA dispersions to enhance $O_2(a^1\Delta_g)$ production. To this end, the hydrophobic porphyrin TPP and, independently, the hydrophilic porphyrin TMPyP were used, both of which are known to produce singlet oxygen in relatively high yield ($\Phi_\Delta \sim 0.7$).[41,48]

We first studied the extent to which the presence of TPP and TMPyP influence the aggregation of HA, ascertaining the location of the porphyrins in the samples. Microscope images of HA suspensions with and without the added porphyrins show the presence of irregularly shaped aggregates with average diameters smaller than 20 μm (Fig. 3). The existence of micrometric humic acids aggregates was previously reported.[49,50] Most importantly, the presence of TMPyP or TPP in the HA suspensions does not appear to affect the size of the HA aggregates. Fluorescence images can be used to help ascertain the extent of porphyrin localization on the HA aggregates. The data show that both TMPyP and TPP are indeed primarily associated with the aggregates (Fig. 3).

Considering a micelle-like structure for the HA aggregates, the cationic porphyrin TMPyP is expected to be bound to the external negatively charged hydrophilic layers of a given aggregate, whereas the more hydrophobic TPP is expected to be mainly located in the interior of the aggregate. Additional experiments were performed to assess this model. HA aggregates to which the respective porphyrins had been added were fixed to the poly-D-lysine base of a microscope cover slip. These samples were then gently washed with neat D_2O or with an HA suspension that did not contain added porphyrin. The washing process was carefully done to avoid the detachment of the aggregate from the cover slips. After washing the samples with D_2O, the fluorescence emission from both the TMPyP- and TPP-containing aggregates did not change (Fig. S2 and S3, ESI†), indicating that the porphyrins remained associated with the aggregates. However, upon washing with the HA suspension, complete removal of TMPyP occurred, whereas TPP remained with the aggregates on the cover slip (Fig. S4 and S5, ESI†). These results strongly suggest that TMPyP is indeed localized on the external surface of the aggregates, and that facile ion exchange with an HA wash can displace these TMPyP molecules from the HA aggregates fixed to the cover slip. On the other hand, TPP in the interior of a given aggregate is not as readily displaced by an HA wash.

A series of microscope-based experiments were performed to further investigate the role of the aggregates on $O_2(a^1\Delta_g)$ kinetics. For this purpose, we employed samples containing one of the porphyrins and focused the irradiating laser beam either on a given HA aggregate or, in a control experiment, on the surrounding bulk phase. The selection of the "correct" aggregate was critical for obtaining a measurable $O_2(a^1\Delta_g)$ phosphorescence signal. In the least, it was necessary to ascertain that the chosen aggregate remained immobile and fixed to the cover slip throughout the

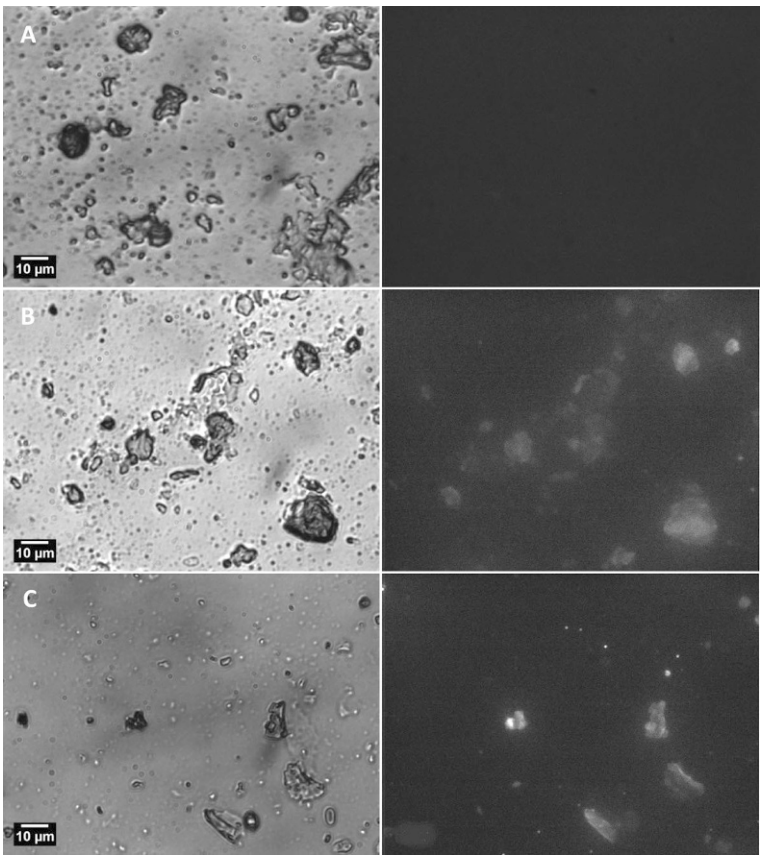

Fig. 3 Bright-field (left) and fluorescence (right) images of the HA aggregates: (A) without added porphyrin; (B) with TMPyP; (C) with TPP.

period of irradiation. In some experiments, bright-field images recorded after the irradiation of the sample revealed a shift of the aggregate from its initial position (Fig. S6, ESI†). In other cases, prolonged irradiation of the aggregate resulted in its partial disaggregation, as shown by the "hole" in the aggregate produced by the laser beam (Fig. S7, ESI†).

In Fig. 4A, we show representative time-resolved 1275 nm $O_2(a^1\Delta_g)$ phosphorescence signals obtained from these microscope-based experiments in which the irradiating laser beam was focused on the aggregate. Given the fundamental differences between this experiment and the cuvette-based experiment, it is not surprising to see differences in the data obtained. Most noticeably, the signal decay constants recorded in the microscope-based experiment are short (*i.e.*, mono-exponential decays with lifetimes of 7.5 μs and 15.1 μs were recorded for HA aggregates containing TPP and TMPyP, respectively) and correspond to those recorded using comparatively high HA concentrations in the cuvette experiments.

Control experiments were performed to further elucidate aspects of the data obtained. With the laser beam focused on the bulk phase of the HA dispersion (*i.e.*, away from a given HA aggregate), we recorded a signal with a lifetime of ~ 7 μs that derives from scattered light-induced detector relaxation (Fig. S8, ESI†).[31] The decay constant obtained from this latter singlet oxygen independent signal is coincident with that measured in the TPP experiment with the laser beam focused on the aggregate (Fig. 4A). Next, HA dispersions containing TPP were irradiated under a N_2-atmosphere with the laser beam focused on single aggregates. The data obtained were the same as those obtained in the presence of an oxygen-containing atmosphere (Fig. S9, ESI†). These control experiments indicate that, under our experimental conditions, the signal with a lifetime of ~7 μs obtained from HA aggregates containing TPP corresponds to a light-induced detector-dependent relaxation and not to $O_2(a^1\Delta_g)$ phosphorescence. In contrast, the time-resolved data obtained from the TMPyP-containing aggregates indicate that the signal observed indeed derives from $O_2(a^1\Delta_g)$ phosphorescence. In particular, upon the addition of NaN_3 to our sample, the comparatively long-lived transient (τ = 15.1 μs) collapses to the shorter-lived transient (τ = 7.4 μs) that we assign to detector relaxation (Fig. 4B).

In summary, in these microscope-based experiments, $O_2(a^1\Delta_g)$ phosphorescence could only be detected from HA aggregates when TMPyP was used as the added sensitizer. This is consistent with our model in which TMPyP is principally localized on the exterior of a given HA aggregate. In this case, an appreciable population of $O_2(a^1\Delta_g)$ thus produced can readily diffuse away from the aggregate into the bulk medium where quenching is not as pronounced. Our inability to detect $O_2(a^1\Delta_g)$ phosphorescence from samples containing TPP is consistent with our model in which, in this case, $O_2(a^1\Delta_g)$ is mainly produced in the interior of the aggregate and is efficiently quenched/deactivated due to the high local concentration of reactive groups in this environment.

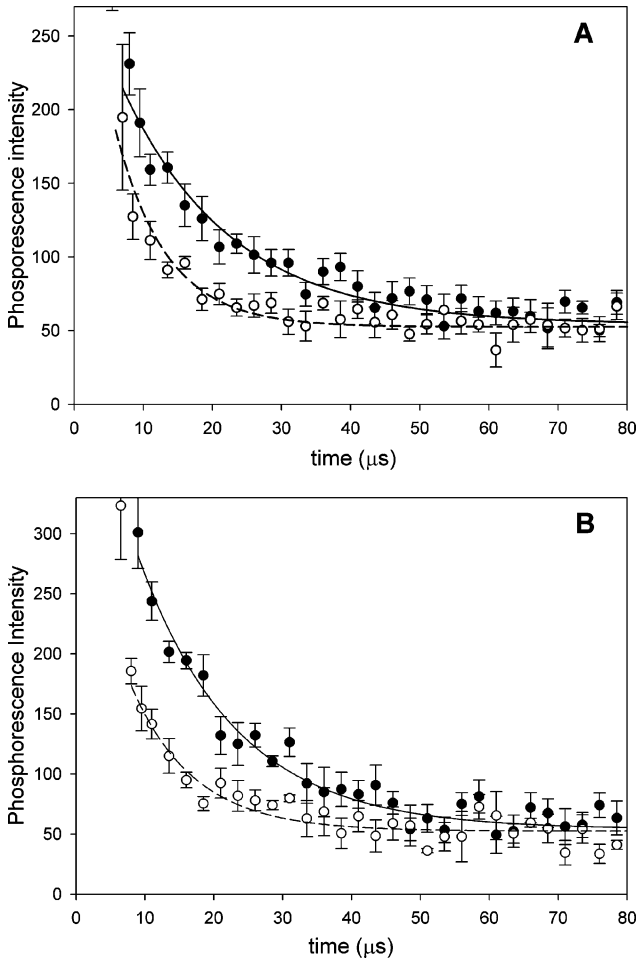

Fig. 4 (A) Comparison between time-resolved $O_2(a^1\Delta_g)$ phosphorescence signals recorded upon focused irradiation of an HA aggregate in a D_2O medium containing TMPyP (●) and, independently, TPP (○). (B) $O_2(a^1\Delta_g)$ phosphorescence data recorded from an HA aggregate containing TMPyP in the absence (●) and presence of NaN_3 (○). The superimposed lines represent exponential fittings of the data.

Conclusion

As far as we know, this is thus far the only study where the effect of the HA micro-aggregation on the singlet oxygen lifetime has been investigated. Given the relative importance of both HA aggregation and the $O_2(a^1\Delta_g)$ lifetime on the photochemistry of aquatic ecosystems, our results should prove useful from a number of perspectives.

One key observation in this study is the fact that the overall rate constant for $O_2(a^1\Delta_g)$ deactivation ($k_q + k_{rxn}$) depends on the HA concentration. Moreover, the data obtained yield a critical concentration for the formation of HA aggregates which is in complete agreement with that determined by monitoring the fluorescence of an added probe (*i.e.*, pyrene). The differences in the rate constant for $O_2(a^1\Delta_g)$ deactivation that depend on the HA concentration appear to reflect the effects that HA aggregation have on sequestering reactive functional groups such that they are less accessible to $O_2(a^1\Delta_g)$.

Both our cuvette and microscope results are consistent with a model in which only the $O_2(a^1\Delta_g)$ molecules which are able to escape from the HA aggregates contribute to the 1275 nm $O_2(a^1\Delta_g)$ phosphorescence signal. We have thus far been unable to provide evidence for a $O_2(a^1\Delta_g)$ phosphorescence signal from inside the aggregates where the $O_2(a^1\Delta_g)$ lifetime seems to be very short and the phosphorescence intensity very weak due, presumably, to the high concentration of reactive groups. This observation suggests that, in natural environments, hydrophobic compounds localized inside HA aggregates, should be somewhat protected against direct photosensitized singlet-oxygen-dependent degradation due to the kinetically competing processes of $O_2(a^1\Delta_g)$ deactivation mediated by the HA itself.

Acknowledgements

This research was supported by ANPCyT, Argentina (PICT 2007 No. 00308), and CICPBA, Argentina. The work at the University of Aarhus was supported by the Danish National Research Foundation through the Center for Oxygen Microscopy and Imaging. L.C. thanks CONICET for a post-doctoral fellowship. D.O.M. is a research member of CICPBA.

References

1 A. Paul, S. Hackbarth, R. D. Vogt, B. Röder, B. K. Burnison and C. E. Steinberg, Photogeneration of singlet oxygen by humic substances: Comparison of humic substances of aquatic and terrestrial origin, *Photochem. Photobiol. Sci.*, 2004, **3**, 273–280.
2 P. R. Ogilby, Singlet oxygen: there is indeed something new under the sun, *Chem. Soc. Rev.*, 2010, **39**, 3181–3209.
3 E. L. Clennan and A. Pace, Advances in singlet oxygen chemistry, *Tetrahedron*, 2005, **61**, 6665–6691.
4 W. J. Cooper, Sunlight induced photochemistry of humic substances in natural waters: major reactive species, *Adv. Chem. Ser.*, 1989, **219**, 332–362.
5 P. M. David Gara, G. N. Bosio, V. B. Arce, L. Poulsen, P. R. Ogilby, R. Giudici, M. C. Gonzalez and D. O. Martire, Photoinduced degradation of the herbicide clomazone model reactions for natural and technical systems, *Photochem. Photobiol.*, 2009, **85**, 686–692.
6 W. R. Haag, J. Hoigne, E. Gassman and A. M. Braun, Singlet oxygen in surface waters - Part II: Quantum yields of its production by some natural humic materials as a function of wavelength, *Chemosphere*, 1984, **13**, 641–650.
7 F. H. Frimmel, H. Bauer, J. Putzien, P. Murasecco and A. M. Braun, Laser flash photolysis of dissolved aquatic humic material and the sensitized production of singlet oxygen, *Environ. Sci. Technol.*, 1987, **21**, 541–545.
8 R. G. Zepp, A. M. Braun, J. Hoigne and J. A. Leenheer, Photoproduction of hydrated electrons from natural organic solutes in aquatic environments, *Environ. Sci. Technol.*, 1987, **21**, 485–490.
9 S. Canonica, Oxidation of aquatic organic contaminants induced by excited triplet states, *Chimia*, 2007, **61**, 641–644.
10 C. Richard, D. Vialaton, J. P. Aguer and F. Andreux, Transformation of monuron photosensitized by soil extracted humic substances: Energy or hydrogen transfer mechanism?, *J. Photochem. Photobiol., A*, 1997, **111**, 265–271.
11 P. P. Vaughan and N. V. Blough, Photochemical formation of hydroxyl radical by constituents of natural waters, *Environ. Sci. Technol.*, 1998, **32**, 2947–2953.
12 W. R. Haag and J. Hoigne, Photo-sensitized oxidation in natural water *via* ·OH radicals, *Chemosphere*, 1985, **14**, 1659–1671.
13 J. V. Goldstone and B. M. Voelker, Chemistry of superoxide radical in seawater: CDOM associated sink of superoxide in coastal waters, *Environ. Sci. Technol.*, 2000, **34**, 1043–1048.
14 N. M. Scully, D. J. McQueen and D. R. S. Lean, Hydrogen peroxide formation: The interaction of ultraviolet radiation and dissolved organic carbon in lake waters along a 43–75°N gradient, *Limnol. Oceanogr.*, 1996, **41**, 540–548.
15 B. Herut, E. Shoham-Frider, N. Kress, U. Fiedler and D. L. Angel, Hydrogen peroxide production rates in clean and polluted coastal

marine waters of the mediterranean red and Baltic seas, *Mar. Pollut. Bull.*, 1998, **36**, 994–1003.
16 M. M. Kononova, *Soil Organic Matter. Its Nature, Its Role in Soil Formation and in Soil Fertility*, Pergamon Press, New York, 1961.
17 R. S. Cameron, R. S. Swift, B. K. Thornton and A. M. Posner, Calibration of gel permeation chromatography materials for use with humic acid, *J. Soil Sci.*, 1972, **23**, 343–349.
18 K. Ghosh and M. Schnitzer, Macromolecular structures of humic substances, *Soil Sci.*, 1980, **129**, 266–276.
19 R. Sutton and G. Sposito, Molecular structure in soil humic substances: The new view, *Environ. Sci. Technol.*, 2005, **39**, 9009–9015.
20 A. Piccolo, The supramolecular structure of humic substances: A novel understanding of humus chemistry and implications in soil science, *Adv. Agron.*, 2002, **75**, 57–134.
21 M. Kerner, H. Hohenberg, S. Ertl, M. Reckermann and A. Spitzy, Self-organization of dissolved organic matter to micelle-like microparticles in river water, *Nature*, 2003, **422**, 150–154.
22 D. E. Latch and K. McNeill, Microheterogeneity of singlet oxygen distributions in irradiated humic acid solutions, *Science*, 2006, **311**, 1743–1747.
23 J. P. Hassett, Dissolved natural organic matter as a microreactor, *Science*, 2006, **311**, 1723–1724.
24 R. L. Malcolm and P. MacCarthy, Limitations in the use of commercial humic acids in water and soil research, *Environ. Sci. Technol.*, 1986, **20**, 904–911.
25 D. A. Backhus and P. M. Gschwend, Fluorescent polycyclic aromatic hydrocarbons as probes for studying the impact of colloids on pollutant transport in groundwater, *Environ. Sci. Technol.*, 1990, **24**, 1214–1223.
26 T. D. Gauthier, E. C. Shane, W. F. Guerin, W. R. Seitz and C. L. Grant, Fluorescence quenching method for determining equilibrium constants for polycyclic aromatic hydrocarbons binding to dissolved humic materials, *Environ. Sci. Technol.*, 1986, **20**, 1162–1166.
27 J. Arnbjerg, M. Johnsen, P. K. Frederiksen, S. E. Braslavsky and P. R. Ogilby, Two-photon photosensitized production of singlet oxygen: Optical and optoacoustic characterization of absolute two-photon absorption cross sections for standard sensitizers in different solvents, *J. Phys. Chem. A*, 2006, **110**, 7375–7385.
28 E. Skovsen, J. W. Snyder, J. D. Lambert and P. R. Ogilby, Lifetime and diffusion of singlet oxygen in a cell, *J. Phys. Chem. B*, 2005, **109**, 8570–8573.
29 E. Skovsen, J. W. Snyder and P. R. Ogilby, Two-photon singlet oxygen microscopy: the challenges of working with single cells, *Photochem. Photobiol.*, 2006, **82**, 1187–1197.
30 M. K. Kuimova, S. W. Botchway, A. W. Parker, M. Balaz, H. A. Collins, H. L. Anderson, K. Suhling and P. R. Ogilby, Imaging intracellular viscosity of a single cell during photoinduced cell death, *Nat. Chem.*, 2009, **1**, 69–73.
31 J. W. Snyder, E. Skovsen, J. D. Lambert, L. Poulsen and P. R. Ogilby, Optical detection of singlet oxygen from single cells, *Phys. Chem. Chem. Phys.*, 2006, **8**, 4280–4293.
32 B. W. Pedersen, T. Breitenbach, R. W. Redmond and P. R. Ogilby, Two-photon irradiation of an intracellular singlet oxygen sensitizer: Achieving localized sub-cellular excitation in spatially-resolved experiments, *Free Radical Res.*, 2010, **44**, 1383–1397.
33 K. Kalyanasundaram and J. K. Thomas, Environmental effects on vibronic band intensities in pyrene monomer fluorescence and their application in studies of micellar systems, *J. Am. Chem. Soc.*, 1977, **99**, 2039–2044.
34 M. Sadoqi, C. A. Lau-Cam and S. H. Wu, Investigation of the micellar properties of the tocopheryl polyethylene glycol succinate surfactants TPGS 400 and TPGS 1000 by steady state fluorometry, *J. Colloid Interface Sci.*, 2009, **333**, 585–589.
35 T. Ohno, Fluorescence inner-filtering correction for determining the humification index of dissolved organic matter, *Environ. Sci. Technol.*, 2002, **36**, 742–746.
36 R. Saxena, S. Shrivastava and A. Chattopadhyay, Exploring the Organization and Dynamics of Hippocampal Membranes Utilizing Pyrene Fluorescence, *J. Phys. Chem. B*, 2008, **112**, 12134–12138.
37 D. Šmejkalová and A. Piccolo, Aggregation and disaggregation of humic supramolecular assemblies by NMR diffusion ordered spectroscopy (DOSY-NMR), *Environ. Sci. Technol.*, 2008, **42**, 699–706.
38 J. Kučerík, D. Šmejkalová, H. Čechlovská and M. Pekař, New insights into aggregation and conformational behaviour of humic substances: Application of high resolution ultrasonic spectroscopy, *Org. Geochem.*, 2007, **38**, 2098–2110.
39 S. Yu. Egorov, V. F. Kamalov, N. I. Koroteev, A. A. Krasnovsky, Jr., B. N. Toleutaev and S. V. Zinukov, Rise and decay kinetics of photosensitized singlet oxygen luminescence in water. Measurements with nanosecond time-correlated single photon counting technique, *Chem. Phys. Lett.*, 1989, **163**, 421–424.
40 P. R. Ogilby and C. S. Foote, Chemistry of singlet oxygen. 36. Singlet molecular oxygen ($^1\Delta_g$) luminescence in solution following pulsed laser excitation. Solvent deuterium isotope effects on the lifetime of singlet oxygen, *J. Am. Chem. Soc.*, 1982, **104**, 2069–2070.
41 F. Wilkinson, W. P. Helman and A. B. Ross, Rate Constants for the Decay and Reactions of the Lowest Electronically Excited Singlet State of Molecular Oxygen in Solution. An Expanded and Revised Compilation, *J. Phys. Chem. Ref. Data*, 1995, **24**, 663–677.
42 A. Michaeli and J. Feitelson, Reactivity of singlet oxygen toward proteins: The effect of structure in basic pancreatic trypsin inhibitor and in ribonuclease A, *Photochem. Photobiol.*, 1997, **65**, 309–315.
43 P. M. D. Gara, G. N. Bosio, M. C. Gonzalez and D. O. Mártire, Kinetics of the sulfate radical-mediated photo-oxidation of humic substances, *Int. J. Chem. Kinet.*, 2008, **40**, 19–24.
44 R. M. Cory, J. B. Cotner and K. McNeill, Quantifying Interactions between Singlet Oxygen and Aquatic Fulvic Acids, *Environ. Sci. Technol.*, 2009, **43**, 718–723.
45 D. P. Hessler, F. H. Frimmel, E. Oliveros and A. M. Braun, Quenching of singlet oxygen ($^1\Delta$(g)) by humic substances, *J. Photochem. Photobiol., B*, 1996, **36**, 55–60.
46 M. A. Rubio, D. O. Mártire, S. E. Braslavsky and E. A. Lissi, Influence of the ionic strength on $O_2(^1\Delta_g)$ quenching by azide, *J. Photochem. Photobiol., A*, 1992, **66**, 153–157.
47 M. Grandbois, D. E. Latch and K. McNeill, Microheterogeneous concentrations of singlet oxygen in natural organic matter isolate solutions, *Environ. Sci. Technol.*, 2008, **42**, 9184–9190.
48 P. K. Frederiksen, S. P. McIlroy, C. B. Nielsen, L. Nikolajsen, E. Skovsen, M. Jørgensen, K. V. Mikkelsen and P. R. Ogilby, Two-Photon Photosensitized Production of Singlet Oxygen in Water, *J. Am. Chem. Soc.*, 2005, **127**, 255–269.
49 P. M. D. Gara, Extraction, characterization of humic substances and its employment in photochemical processes of environmental interest, *PhD Thesis*, National University of La Plata, 2008.
50 M. Baalousha, M. Motelica-Heino and P. L. Coustumer, Conformation and size of humic substances: Effects of major cation concentration and type, pH, salinity, and residence time, *Colloids Surf., A*, 2006, **272**, 48–55.

